Implementation of a semiclassical light-matter interaction using the Gauss-Hermite quadrature: A simple alternative to the multipole expansion

Lasse Kragh Sørensen,[1,*] Emil Kieri,[2,†] Shruti Srivastav,[1,‡] Marcus Lundberg,[1] and Roland Lindh[1,§]
[1]*Department of Chemistry, Ångström Laboratory, Uppsala University, Box 538, SE-75121 Uppsala, Sweden*
[2]*Division of Scientific Computing, Department of Information Technology, Uppsala University, Box 337, SE-75105 Uppsala, Sweden*

(Received 24 September 2018; published 16 January 2019)

We present an analytical and numerical solution of the calculation of the transition moments for the exact semiclassical light-matter interaction for wave functions expanded in a Gaussian basis. By a simple manipulation we show that the exact semiclassical light-matter interaction of a plane wave can be compared to a Fourier transformation of a Gaussian where analytical recursive formulas are well known and hence, making the difficulty in the implementation of the exact semiclassical light-matter interaction comparable to the transition dipole. Since the evaluation of the analytical expression involves a new Gaussian, we instead have chosen to evaluate the integrals using a standard Gauss-Hermite quadrature, since this is faster. A brief discussion of the numerical advantages of the exact semiclassical light-matter interaction in comparison to the multipole expansion along with the unphysical interpretation of the multipole expansion is discussed. Numerical examples on $[CuCl_4]^{2-}$ show that the usual features of the multipole expansion are immediately visible also for the exact semiclassical light-matter interaction and that this can be used to distinguish between symmetries. Calculation on $[FeCl_4]^{1-}$ is presented to demonstrate the better numerical stability with respect to the choice of basis set in comparison to the multipole expansion and finally, Fe-O-Fe to show origin independence is a given for the exact operator. The implementation is freely available in OpenMolcas.

DOI: 10.1103/PhysRevA.99.013419

I. INTRODUCTION

Over the years a large variety of spectroscopies have been developed which has given a great understanding of molecules and materials from basic characterization [1]. All spectroscopies, until recently [2], have come from the interaction between external or internal electromagnetic fields. While a great deal of information can be extracted from experimental spectra alone, the more detailed correspondence between observed properties and molecular structures is often better illuminated when experimental results are combined with theoretical results, since individual transitions can be separated.

In reconstructing the experimental spectra from theory it is necessary to introduce the given external electromagnetic fields in the description of the molecular system. The external fields used in the different types of spectroscopy are often weak in comparison to the atomic fields, or do not significantly perturb the system before measurement, and can therefore be treated classically [3–5] and as a perturbation. Usually, for laser fields, the electromagnetic field is described by a plane wave where the vector potential is a complex exponential function. Traditionally, a multipole expansion is introduced and truncated at some finite order to describe the interaction of the external electromagnetic field with the system. The first term in this multipole expansion is the electric dipole, and the next term that is included is typically the electric quadrupole, followed by other magnetic and electric multipoles. While simple, the higher-order terms depend on the choice of origin for the multipole expansion, at least in cases where there are nonzero terms of lower order. For weak fields, which can be treated as a perturbation, the problem of origin dependence was recently solved by Bernadotte *et al.* [6], simply by truncating the multipole in the observable wave vector and not in the nonobservable transition moments traditionally done. A complete expansion to the second order, most commonly associated with electric quadrupole, then requires calculations up to magnetic quadruples and electric octupoles.

Bernadotte *et al.* [6] showed that origin dependence is exact when using the velocity gauge. We later showed that origin independence in a finite basis set can also be accomplished in the length gauge, but what is typically referred to as the length gauge is actually a mixed gauge, with the electric and magnetic components in the length and velocity gauges, respectively [7]. Origin independence, in finite basis sets, is not conserved in this mixed gauge [8]. Furthermore, the increased basis set requirement and convergence behavior for every order in the multipole expansion cannot be overlooked [8,9].

An alternative way to evaluate the oscillator strengths is to simply use the exact semiclassical light-matter interaction and not perform any multipole expansion. In this way there will only be one type of integrand that needs to be evaluated and not, like for the multipole expansion, many integrands with different basis set requirements. Only recently have exact

*lasse.kragh.soerensen@gmail.com
†Institut für Numerische Simulation, Wegelerstrasse 6, DE-53115 Bonn, Germany.
‡COMSOL AB, Tegnérgatan 23, SE-111 40 Stockholm, Sweden.
§Uppsala Center of Computational Chemistry -UC_3, Uppsala University, Box 538, SE-75121 Uppsala, Sweden.

semiclassical light-matter interactions of a plane wave been implemented [10,11], along with the dynamic structure factors [12], which from a numerical viewpoint are very similar. A possible reason for the delay in the implementation is that the evaluation of the integrals for the exact semiclassical light-matter interaction have been described as being very difficult and a major obstacle in the evaluation of the operator [6,12]. However, the integrals Lehtola *et al.* [12] encounters, which are like those for the exact semiclassical light-matter interaction, can actually be solved by using the closure property of Gaussians and directly computing the values of the Fourier transforms. Still, in the previous implementations either a number of new recursive relations need to be programed along with the need to introduce trigonometric functions [10,11], or a Fourier transformation of the overlap between basis functions should be performed [12]. We, however, intend to show that the evaluation of the integrals for the exact semiclassical light-matter interaction in a Gaussian basis set is even simpler and can be performed using either analytical formulas or standard integral evaluation methods in quantum chemistry.

Seeing the ease with which the integrals for the exact semiclassical light-matter interaction can be implemented both here and in other codes [10–12], in comparison to the higher orders of the multipole expansion and the numerical and origin dependence problems of the multipole expansion, we no longer see the need for implementing the multipole expansion for the evaluation of transition moments.

To illustrate the behavior of the exact operator, we will perform calculations with high-energy photons, which corresponds to large k vectors, rapidly oscillating fields, and thus larger relative intensity of higher-order terms in the plane-wave expansion. In x-ray absorption spectroscopy (XAS), the K edge of first-row transition metals, typically associated with electric dipole-allowed $1s$ to $4p$ transitions, uses photon energies of thousands of eV. Before the rising edge, there are weaker pre-edge transitions assigned to $1s$ to $3d$ transitions, which provides insight into the nature of the bonding between the transition metal(s) and ligands [13–15]. Since the $1s$ to $3d$ is dipole forbidden in centrosymmetric environments, higher-order terms in the multipole expansion must be included in order to describe these transitions, or by using the exact operator [11].

The x-ray calculations will be performed using the restricted active space (RAS) method, which is a multiconfigurational wave-function approach [16,17]. RAS has been successfully applied to simulate L-edge XAS and resonant inelastic x-ray scattering (RIXS) of several transition-metal systems [18–20]. We have also implemented the second-order expansion of the wave vector to describe XAS and RIXS in the K pre-edge [21,22].

The presented examples all represent cases with weak electromagnetic fields. However, in past decades, with the advent of very short and brilliant laser pulses the perturbative treatment can break down in and one enters the strong-field regime where the external and atomic field must treated on equal footing and a dynamical treatment is necessary [3–5]. For strong fields, beyond the dipole approximation, the problem of origin dependence still persists for the multipole expansion. We will here allude to how the work on the exact semiclassical light-matter interaction can be carried directly over to the strong-field regime because all interaction terms can be evaluated using the same simple integrals. This means that the method also could be used in simulations of dynamics of molecules in strong electric and magnetic fields, and this, we believe, is where the real strength of the approach may lie.

For self-consistency we will in Sec. II A recapitulate the perturbative treatment of molecules in weak electromagnetic fields and the multipole expansion. Thereafter, in Sec. II B we will show how the integrals for the exact semiclassical light-matter interaction can be evaluated using standard quantum chemistry integral programs, followed by the isotropically averaged oscillator strengths in Sec. II B 1. For the applications in Sec. III we demonstrate the advantage of using the exact semiclassical light-matter interaction instead of the multipole expansion on different systems, which has been problematic with the multipole-expansion approach. A perspective on and the possibility of dynamics simulations with the exact semiclassical light-matter interaction is given in Sec. IV A and finally a summary and conclusion in Sec. V.

II. THEORY

In the first of the two parts of this section we will briefly discuss the well-known formulas for the semiclassical light-matter interaction and how the oscillator strengths usually are calculated from perturbation theory along with a short discussion of the unphysical interpretation of the multipole expansion often seen. In the second part we will show the how integrals for the exact semiclassical light-matter interaction can be evaluated analytically, along with an easy way to compute the integrals using a standard Gauss-Hermite quadrature. Finally, the isotropic averaging of the exact semiclassical light-matter interaction is mentioned.

A. Perturbation from weak fields

Throughout this section it is assumed that the electromagnetic fields are weak and therefore can be treated as a perturbation of the molecular system. The zeroth-order Hamiltonian, in our case, is the Schrödinger equation within the Born-Oppenheimer approximation,

$$\hat{H}_0 = \sum_{i=1}^{N} \frac{\hat{\boldsymbol{p}}_i^2}{2m_e} + V(\boldsymbol{r}_1, \ldots, \boldsymbol{r}_N), \tag{1}$$

which is exposed to a time-dependent perturbation $\hat{U}(t)$:

$$\hat{U}(t) = -\frac{e}{m_e c} \sum_i \boldsymbol{A}(\boldsymbol{r}_i, t) \cdot \hat{\boldsymbol{p}}_i + \frac{e^2}{2m_e c^2} \boldsymbol{A}^2(\boldsymbol{r}_i, t) - \frac{ge}{2m_e c} \sum_i \boldsymbol{B}(\boldsymbol{r}_i, t) \cdot \hat{\boldsymbol{s}}_i \tag{2}$$

$$= \frac{eA_0}{2m_e c} \sum_i \Big[\exp(\imath(\boldsymbol{k} \cdot \boldsymbol{r}_i - \omega t))(\boldsymbol{\mathcal{E}} \cdot \hat{\boldsymbol{p}}_i) \tag{3}$$

$$+ \frac{eA_0}{4c} (\exp(2\imath(\boldsymbol{k} \cdot \boldsymbol{r}_i - \omega t)) + 1) \tag{4}$$

$$+ \imath \frac{g}{2} \exp(\imath(\boldsymbol{k} \cdot \boldsymbol{r}_i - \omega t))(\boldsymbol{k} \times \boldsymbol{\mathcal{E}}) \cdot \hat{\boldsymbol{s}}_i + \text{c.c.} \Big], \tag{5}$$

from a monochromatic linearly polarized electromagnetic wave where $\boldsymbol{k}$ is the wave vector pointing in the direction of propagation, $\boldsymbol{\mathcal{E}}$ the polarization vector perpendicular to $\boldsymbol{k}$, ω is the angular frequency, $\hat{\boldsymbol{s}}$ the spin, A_0 the amplitude of the vector potential, $\boldsymbol{B}$ the magnetic field, and c.c. the complex conjugate of the previous terms.

Of the terms in Eqs. (3)–(5), often the dipole approximation is taken, meaning that only the zeroth-order term in the vector potential ($\boldsymbol{A}$) in Eq. (3) is included

$$\exp(\imath \boldsymbol{k}\cdot\boldsymbol{r}_i) = 1 + \imath(\boldsymbol{k}\cdot\boldsymbol{r}_i) - \tfrac{1}{2}(\boldsymbol{k}\cdot\boldsymbol{r}_i)^2 + \cdots . \tag{6}$$

While the dipole approximation suffices for optical transitions, for analyzing the K edge x-ray spectroscopy terms up to second order must be included. The ($\boldsymbol{A}^2$) in Eq. (4) is mostly relevant for strong fields and will always depend explicitly on the field strength A_0, which makes little sense for weak fields, treated perturbatively, where this dependence is removed from the terms in Eqs. (3) and (5). Equation (5) describes the interaction between the spin and the magnetic field and is relevant when describing open-shell transitions. Furthermore, the values of all terms in Eqs. (3)–(5) also depend on the choice of gauge, though the sum is constant. In the Coulomb gauge, which is the usual choice in molecular physics, ($\boldsymbol{A}^2$) has a minimum [23] and will be neglected in the applications.

Using Fermi's golden rule, transitions only occur when the energy difference between the eigenstates of the unperturbed molecule matches the frequency of the perturbation,

$$\omega = \omega_{0n} = \frac{E_n - E_0}{\hbar}, \tag{7}$$

and the explicit time dependence can be eliminated from the transition rate

$$\Gamma_{0n}(\omega) = \frac{2\pi}{\hbar}|\langle 0|\hat{U}|n\rangle|^2\delta(\omega-\omega_{0n}) = \frac{\pi A_0^2}{2\hbar c}|T_{0n}|^2\delta(\omega-\omega_{0n}). \tag{8}$$

Now the effect of the weak electromagnetic field can be expressed as a time-independent expectation value. From Eq. (8) the relation between the transition moments T_{0n} and the time-independent part $\hat{U}$ of $\hat{U}(t)$ in Eq. (2) is seen. From the transition moments T_{0n} and the oscillator strengths f_{0n},

$$f_{0n} = \frac{2m_e}{e^2 E_{0n}}|T_{0n}|^2, \tag{9}$$

where $E_{0n} = E_n - E_0$ is the difference in the energy of the eigenstates of the unperturbed molecule and can then be calculated. The amplitude of the electric and magnetic field $E_0 = B_0 = A_0 k$ or intensity therefore does not have to be defined for Eqs. (3) and (5), while for the quadratic $\boldsymbol{A}^2$ term in Eq. (4) the amplitude is still needed.

Traditionally, a multipole expansion of the exponential function of the perturbation in Eq. (2) is performed, which gives rise to the nonobservable electric and magnetic dipole, and quadrupole and higher-order approximations for the transition moments T_{0n}. Unfortunately, such an expansion in the transition moments T_{0n} is only origin independent for the dipole and in the limit of a complete expansion.

Origin independence, however, appears naturally, provided that the collection of the terms in Taylor expansion of the exponential of the wave vector $\boldsymbol{k}$ in Eq. (2) are collected to the same order in the observable oscillator strengths,

$$\begin{aligned} f_{0n} &= f_{0n}^{(0)} + f_{0n}^{(1)} + f_{0n}^{(2)} + \cdots \\ &= \frac{2m_e}{e^2 E_{0n}}\left|T_{0n}^{(0)} + T_{0n}^{(1)} + T_{0n}^{(2)} + \cdots\right|^2, \end{aligned} \tag{10}$$

as shown by Bernadotte *et al.* [6]. Lestrange *et al.* [24] demonstrated that collecting the terms in the oscillator strengths according to Eq. (10) does not always ensure a positive total oscillator strength when truncating the expansion, since the perfect square of the transition moments is broken. The total negative oscillator strengths when truncating Eq. (10) appear to be a basis set problem that can occur for unbalanced basis sets for some transitions [8].

While the truncation in the oscillator strength eliminates the problem of origin dependence, the multipole expansion, however, introduces an increasing demand on the basis set for every order in the expansion, since the integrand changes for every order [9]. This means that in order to calculate the K pre-edge peaks in an x-ray spectrum, the basis set must be able to accurately describe all terms at least up to second order in the transition moment, i.e., the electric octupole and magnetic quadrupole terms. While the higher-order terms could be expected to be small, these can be grossly overestimated in some basis sets [8].

The multipole expansion can be a useful model, because in some systems it gives selection rules that can be used to rationalize the relative strength of different transitions, which in turn aids the interpretation between spectra and electronic structure. As an example, for $1s$ excitations in metal K edges of mononuclear metal centers, the electric quadrupole component can be related to transitions involving the metal $3d$ orbitals [14]. However, it should be noted that none of the terms in the multipole expansion in Eq. (10) are individually observable. The same argument also goes for the origin-independent oscillator strengths [6], which despite their origin independence, still are not individually observable. Trying to interpret spectra in terms of the different orders in the multipole expansion or even as electric or magnetic is not physical, since only the total can be observed and changes of coordinate system can significantly alter the interpretation [8]. Therefore the selection rules traditionally derived and used to explain spectra are dependent on the choice of coordinate system. With an origin-independent approach the selection rules can still be used to aid in the interpretation of electronic structure by separating transitions into relative strengths according to the zeroth and second order of the oscillator strengths. We here note that even though a second-order transition may be several orders of magnitude weaker than a zeroth order, the individual terms in the second order can still be significantly larger than the dipole contribution in an actual calculation due to the origin dependence of these terms [8].

B. Evaluation of the integrals for the exact semiclassical light-matter interaction

The evaluation of the integrals for the exact semiclassical light-matter interaction has been the major obstacle in the evaluation of the operator [6,12]. We will show that the exact

semiclassical light-matter interaction of a plane wave can be thought of as a Fourier transformation of the overlap between basis functions and that this can be solved analytically. In the Gaussian basis sets we use just these results in a new Fourier-transformed Gaussian. The evaluation of the integrals are therefore very similar to those found for the overlap and operators in a Gaussian plane-wave basis set [25–27], and similarities are shared with the plane-wave representations of the electromagnetic field [28].

In order to evaluate Eq. (8), for the perturbation in Eq. (2) the matrix element

$$\langle 0|\hat{U}|n\rangle = \sum_{\mu\nu} U_{\mu\nu}^{AB} \gamma_{\mu\nu}^{AB} \tag{11}$$

must be calculated. In Eq. (11) $U_{\mu\nu}^{AB}$ is the integral matrix for the orbital bases A and B, with indices μ and ν and likewise defined for the transition density matrix $\gamma_{\mu\nu}^{AB}$ [29]. For a wave function expanded in Gaussians, the individual terms in $U_{\mu\nu}^{AB}$ from Eq. (3) correspond to evaluating integrals of the form

$$I = \langle \chi_\mu | e^{\pm \imath \boldsymbol{k}\cdot\boldsymbol{r}} \hat{\boldsymbol{p}} | \chi_\nu \rangle, \tag{12}$$

where the real-valued atomic Cartesian basis functions χ_μ and χ_ν are expressed as

$$\chi_\mu(\boldsymbol{r}) = \chi_{i,j,k}(\boldsymbol{r}, \alpha_\mu, \boldsymbol{A}) \tag{13}$$

$$= (x - A_x)^i (y - A_y)^j (z - A_z)^k e^{-\alpha_\mu \|\boldsymbol{r} - \boldsymbol{A}\|^2} \tag{14}$$

$$= \chi_i(x, \alpha_\mu, A_x)\chi_j(y, \alpha_\mu, A_y)\chi_i(z, \alpha_\mu, A_z) \tag{15}$$

in their different components, where i, j, and k represent the order of the Cartesian components x, y, and z, respectively. The integral in Eq. (12) can be factorized into three one-dimensional integrals,

$$I_x = \int_{-\infty}^{\infty} \chi_i(x, \alpha_\mu, A_x) e^{\pm \imath k_x x} \hat{p}_x \chi_j(x, \alpha_\nu, B_x) dx. \tag{16}$$

Applying the differentiation operator $\hat{p}_x = -\imath\hbar\frac{\partial}{\partial x}$, we find

$$I_x = -\imath\hbar\epsilon_x \int_{-\infty}^{\infty} \chi_i(x, \alpha_\mu, A_x) e^{\pm \imath k_x x} (j\chi_{j-1}(x, \alpha_\nu, B_x) - 2\alpha_\nu \chi_{j+1}(x, \alpha_\nu, B_x)) dx, \tag{17}$$

that the integral I_x can be expressed as a sum of two terms. From Eq. (17) it is seen that both terms are of the form

$$\int_{-\infty}^{\infty} e^{\pm \imath k_x x} \chi_i(x, \alpha_\mu, A_x)\chi_j(x, \alpha_\nu, B_x) dx. \tag{18}$$

Using the Gaussian product formula, we see that the expression in Eq. (18) is akin to a Fourier transformation of a Gaussian from real space x to k_x space. Integrals of the from in Eq. (18) can be solved analytically using recursive formulas for the analytical Fourier representation of Gaussians [25]. Equation (18) can also be viewed as the Fourier transformation of the overlap between two basis functions, as also noted by Lehtola *et al.* [12].

Since the Fourier transformation of a Gaussian is a new Gaussian, we have chosen not to use the analytical form but instead rewrite the integral in Eq. (18) to a form which easily can be evaluated by a standard Gauss-Hermite quadrature. Using the Gaussian product formula of Eq. (18),

$$I'_x = \int_{-\infty}^{\infty} e^{\pm \imath k_x x} \chi_i(x, \alpha_\mu, A_x)\chi_j(x, \alpha_\nu, B_x) dx \tag{19}$$

$$= e^{-\frac{\alpha_\mu\alpha_\nu}{\zeta}(A_x - B_x)^2} \int_{-\infty}^{\infty} (x - A_x)^i (x - B_x)^j e^{-\zeta(x - P_x)^2 \pm \imath k_x x} dx, \tag{20}$$

where $\zeta = \alpha_\mu + \alpha_\nu$ and $P_x = (\alpha_\mu A_x + \alpha_\nu B_x)/\zeta$, we can complete the square in the exponent

$$I'_x = e^{-\frac{\alpha_\mu\alpha_\nu}{\zeta}(A_x - B_x)^2} e^{\gamma} \int_{-\infty}^{\infty} (x - A_x)^i (x - B_x)^j e^{-\zeta(x - Q_x)^2} dx, \tag{21}$$

where $Q_x = P_x \pm \imath k_x/(2\zeta)$ and $\gamma = \zeta(Q_x^2 - P_x^2)$. We here notice that for a mixed Gaussian plane-wave basis set, expressions similar to Eq. (20) for an overlap appear [27].

Making a change of variables $z = \sqrt{\zeta}(x - Q_x)$, the integral in Eq. (21) can now be transformed to

$$I'_x = \Theta \lim_{R\to\infty} \int_{-z=\sqrt{\zeta}(R-Q_x)}^{z=\sqrt{\zeta}(R-Q_x)} \left(\frac{z}{\sqrt{\zeta}} + Q_x - A_x\right)^i \times \left(\frac{z}{\sqrt{\zeta}} + Q_x - B_x\right)^j e^{-z^2} dz, \tag{22}$$

where

$$\Theta = e^{-\frac{\alpha_\mu\alpha_\nu}{\zeta}(A_x - B_x)^2} e^{\gamma}/\sqrt{\zeta}. \tag{23}$$

Defining the polynomial

$$f(z) = \Theta\left(\frac{z}{\sqrt{\zeta}} + Q_x - A_x\right)^i \left(\frac{z}{\sqrt{\zeta}} + Q_x - B_x\right)^j, \tag{24}$$

Eq. (22) can be written a little more compactly,

$$I'_x = \lim_{R\to\infty} \int_{-z=\sqrt{\zeta}(R-Q_x)}^{z=\sqrt{\zeta}(R-Q_x)} f(z) e^{-z^2} dz. \tag{25}$$

Since the integral in Eq. (25) is analytic, the integration is independent of the path and can therefore be split into

$$I'_x = \lim_{R\to\infty} \int_{-z=\sqrt{\zeta}(R-Q_x)}^{z=\sqrt{\zeta}R} f(z) e^{-z^2} dz \tag{26}$$

$$+ \lim_{R\to\infty} \int_{-z=\sqrt{\zeta}R}^{z=\sqrt{\zeta}R} f(z) e^{-z^2} dz \tag{27}$$

$$+ \lim_{R\to\infty} \int_{-z=\sqrt{\zeta}R}^{z=\sqrt{\zeta}(R-Q_x)} f(z) e^{-z^2} dz. \tag{28}$$

Since $\sqrt{\zeta} > 0$ and the exponential decay of the integrand as $\Re_z \to \pm\infty$, two of the integrals vanish, leaving

$$I'_x = \lim_{R\to\infty} \int_{-z=\sqrt{\zeta}R}^{z=\sqrt{\zeta}R} f(z) e^{-z^2} dz = \int_{-\infty}^{\infty} f(z) e^{-z^2} dz, \tag{29}$$

for which the Gauss-Hermite quadrature is designed to compute. Since z is complex the Gauss-Hermite quadrature must use complex numbers. With the standard Gauss-Hermite

nodes z_n and weights w_n, we compute the integral as

$$I'_x = \sum_n w_n f(z_n), \tag{30}$$

or equivalently, with the transformed quadrature nodes $x_n = z_n/\sqrt{\zeta} + Q_x$,

$$I'_x = \Theta \sum_n w_n (x_n - A_x)^i (x_n - B_x)^j. \tag{31}$$

The total integral in Eq. (12) can therefore simply be written as a triple product of the cartesian components

$$I = I'_x * I'_y * I'_z. \tag{32}$$

Due to the similarities between the electric term in the exact semiclassical light-matter interaction for a plane wave [Eq. (3)], with the quadratic and magnetic terms [Eqs. (4) and (5)] all these integrals can be evaluated in exactly the same manner. All three terms are therefore programed in OpenMolcas [30]. The coupling between the magnetic field and the spin in Eq. (5) is only nonzero when the spin-magnetic-field operator in the RASSI module [31] is used. Equation (4) also gives a constant nonzero contribution in all directions, but since Eq. (4) still depends explicitly on the field strength, we have neglected this term since for the field strengths needed for Eq. (4) to be influential the perturbative treatment of the light-matter interaction will break down.

The resulting formulas are not surprisingly like those found using Gauss-Rys quadrature in a Gaussian plane-wave basis set as derived by Čarsky and Polášek [26] and does not require any new recursive relations or expansion in trigonometric functions as in previous implementations [10,11]. Finally, it is noted we have here demonstrated that the target integrals can be computed by a standard Gauss-Hermite quadrature using complex numbers for z while the roots and weights are still real. It has in the past been demonstrated, for two-electron integrals, that there is a direct relation between an exact quadrature and an integral recursive procedure—in this case the Gauss-Rys quadrature and the McMurchie-Davidson scheme [32]. In line with this, it is reasonable to expect that an extension of the original McMurchie-Davidson scheme, for one-electron overlap integrals, to complex numbers, as in the case of the Gauss-Hermite quadrature, would be sufficient for the computation of the target integrals.

1. Isotropically averaged oscillator strengths

For the terms in the multipole expansion, well known isotropically tensor averaged oscillator strengths can be found in literature [33]. For the exact expression no closed formula exists. Lebedev and co-workers [34–39] have devised a way of distributing quadrature points over a unit sphere defining a Lebedev grid, which gives the propagation directions included in the numerical integration for the incoming light. By averaging over two orthogonal polarization directions for the different directions for the propagation the exact isotropic average can be systematically approximated. List *et al.* [11] have shown that this converges very rapidly with the number of quadrature points, and we therefore have also adopted the Lebedev grid for the isotropic averaging.

While the exact semiclassical light-matter interaction is cheaper to calculate than the second-order quadrupole intensities for a single direction for the isotropic averaging, the cost is approximately the same due to the tensor averaging in the multipole expansion.

III. APPLICATION

In this section we will study the metal K pre-edge XAS of two molecular systems, $[CuCl_4]^{2-}$ and $[FeCl_4]^{1-}$, as well as the iron dimer model complex $[Fe_2O]^{4+}$, to highlight properties specific to the use of the exact semiclassical operator versus standard multipole techniques. In a classical experiment, the angular dependence of the pre-edge intensity of single-crystal $[CuCl_4]^{2-}$ was used to identify the electric quadrupole contribution and to identify the symmetry of the singly occupied $3d$ orbital. In general, the assignment of transitions to different multipole contributions has helped to connect spectra to the electronic structure. With the $[CuCl_4]^{2-}$ example, we will demonstrate how the exact operator reproduces the behavior of what is traditionally referred to as an electric quadrupole transition.

As mentioned above, electric quadrupole transitions are origin-dependent if the electric dipole contributions are nonzero. $[FeCl_4]^{1-}$ has tetrahedral symmetry, and the noncentrosymmetric ligand environment leads to intense dipole contributions and strong contributions from many terms in the full second-order expansion [6,8,21]. For some basis sets, the expansion even leads to unphysical negative oscillator strengths [7,8,24]. These examples are revisited with the exact semiclassical operator to show its stability in incomplete basis sets.

Finally, we address an iron dimer where there is no natural choice of the origin for the multipole expansion of an iron-centered transition. We show the origin independence of the exact operator by comparing the results for $[Fe_2O]^{4+}$ to previous calculations using the multipole expansion in the mixed gauge. However, before that we describe the computational details.

A. Computational details

The geometry of the $[CuCl_4]^{2-}$ is taken from the x-ray crystal structure [14]. The complex has a square planar geometry, formal D_{2h} symmetry, with Cu-Cl bond lengths of 2.233 and 2.268 Å, and Cl-Cu-Cl angles of 89.91° and 90.09°. The short bonds were placed along the x axis. To show the effect of the angles, another calculation in D_{2h} symmetry with Cl-Cu-Cl angles of 90° and with all bonds along the x and y axis, here labeled $D_{2h\perp}$, were also performed. Finally, calculations were made in D_{4h} symmetry using an average bond length of 2.2505 Å.

The geometry of $[FeCl_4]^{1-}$ is also taken from an x-ray structure [40]. The ligand environment is tetrahedral (T_d point group), with four Fe-Cl distances of 2.186 Å. The geometry of Fe-O-Fe is taken from a BP86/6-311(d) geometry optimization of [(hedta)FeOFe(hedta)], which gives C_{2v} symmetry, Fe-O distances of 1.76 Å, and an angle of 148 degrees [8].

Orbital optimization is performed using state-average RASSCF, with separate optimizations for ground and

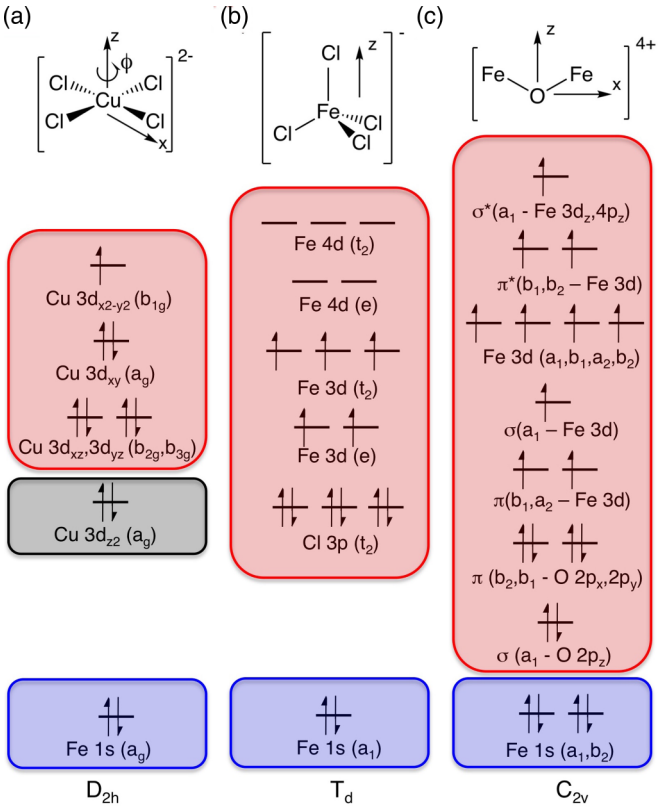

FIG. 1. Ligand geometries and active spaces for metal K pre-edge XAS modeling of (a) $[CuCl_4]^{2-}$, (b) $[FeCl_4]^{1-}$, and (c) $[Fe_2O]^{4+}$.

core-excited states as implemented in OpenMolcas [30]. In all calculations the metal $1s$ orbitals are included in RAS1, constraining to at most one hole. For the calculations of the core excited states, the weights of all configurations with fully occupied $1s$ orbitals have been set to zero. To avoid orbital rotation, i.e., the hole appears in a higher-lying orbital, the $1s$ orbitals have been frozen in the calculation of the final states.

$[CuCl_4]^{2-}$ is a formal $3d^9$ complex with a singly occupied $3d_{x2-y2}$ orbital, leading to a doublet ground state. We focus only on the $1s \rightarrow 3d_{x2-y2}$ transition and use a small RAS2 space, including seven electrons in four metal-centered orbitals (see Fig. 1). Due to weak spin-orbit coupling, only final states of the same spin multiplicity as the ground state are considered in the calculations. For $[CuCl_4]^{2-}$ only one doublet core excited state is necessary to include.

$[FeCl_4]^{1-}$ is a high-spin $3d^5$ complex with a sextet ground state. The calculations are similar to those laid out in previous works [7,8], with 11 electrons in 13 orbitals in RAS2, see Fig. 1. The orbitals of the sextet excited states were averaged over 70 states.

The ground state of the iron dimer $[Fe_2O]^{4+}$ is a singlet with five unpaired electrons on each ferric iron coupled antiferromagnetically. To facilitate RASSCF convergence, calculations are instead performed with ferromagnetic coupling, giving undetected states. The RAS2 space consists of the three $2p$ orbitals of the bridging oxygen and the ten $3d$ orbitals of the irons, which gives a total of 16 electrons in 13 orbitals, see Fig. 1. Sixty core-excited states were used, exactly like in previous work [8].

For the correlation treatment all calculations will be at the RASSCF level, as inclusion of dynamical correlation on the behavior of the transitions can be assumed to be minor. Scalar relativistic effects have been included by using a second-order Douglas-Kroll-Hess Hamiltonian in combination with the ANO-RCC-VTZP basis set [41–44]. This basis set has been shown to perform reasonably well for both electronic structure and for the transition moments [8]. The intensities for the exact operator and the quadrupole intensities in the mixed gauge are implemented in the RASSI program [31,45] and distributed freely in the OpenMolcas package [30]. Simulated spectra are plotted using a Lorentzian lifetime broadening with a FWHM of 1.25 eV and further convoluted with a Gaussian experimental broadening of 1.06 eV.

B. Assignment of K pre-edge XAS contributions for $[CuCl_4]^{2-}$

Metal K pre-edges are weak transitions on the low-energy side of the rising edge. They are typically assigned to $1s \rightarrow 3d$ transitions. In centrosymmetric geometries these are electric dipole forbidden and only gain intensity through what is typically referred to as electric quadrupole transitions. However, vibronic coupling with normal modes that break centrosymmetry allow for electric dipole contributions also for complexes with formal centrosymmetry.

In single crystals the orientation of the molecule with respect to the beam can be controlled. The angular dependence of the normalized peak heights in the Cu K pre-edge of $[CuCl_4]^{2-}$, taken from Ref. [14], is shown in Fig. 2(a). The angle ϕ shows rotation around the molecular z axis, with 0° representing the direction of the electromagnetic k vector relative to the short Cu-Cl bond. The electric quadrupolar contribution is distinguished by a fourfold periodicity of the cross section. The highest intensity is observed for orientations bisecting the Cu-Cl bond, which makes it possible to assign the half-filled orbital to be $3d_{x2-y2}$ [14]. The isotropic contribution is assigned to an electric dipole contribution that gains intensity through vibronic coupling.

The angular dependence of the oscillator strengths calculated using the exact operator is shown in Fig. 2(b). The fourfold periodicity is reproduced, which is a simple illustration that the exact operator reproduces the observables that have been traditionally used to assign transitions to different multipole components. The isotropic contributions are missing from the calculated spectra simply because vibronic coupling is not taken into account in our calculations.

In the real complex the Cu-Cl bonds are not perfectly symmetric. In order to see the very slight asymmetry in the angular spectrum of $[CuCl_4]^{2-}$, one needs to explicitly compare the oscillator strengths on both sides of the peaks, e.g., 130° and 140°. Due to the lack of data points and reasonably large error bars in the experiment, distortions from D_{4h} are difficult to quantify in the experimental spectrum. In Table I the peak and minimum along with their neighboring values are listed to show the asymmetry in the spectrum of $[CuCl_4]^{2-}$ and how little the values change with nuclear geometry. From Table I it is seen that the difference between the points next to the peak and minimum is a mere $1.0 * 10^{-8}$ for D_{2h}, which, of course, is much lower than the accuracy of the calculation but still above numerical noise. For D_{4h} the difference between

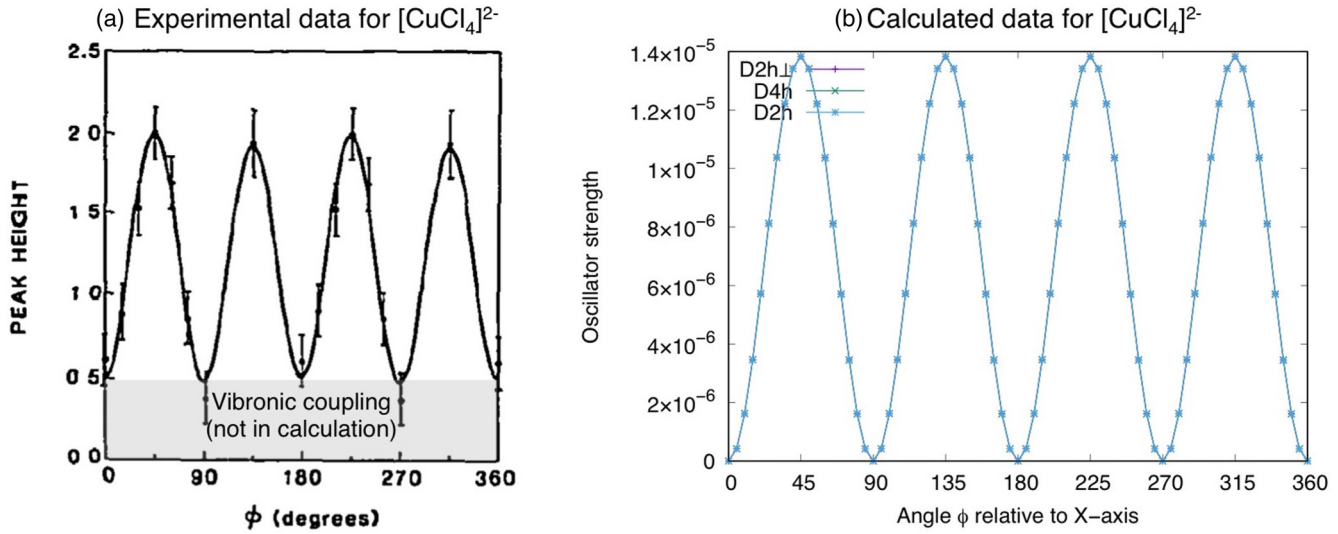

FIG. 2. Experimental and calculated angular dependence of the K pre-edge transition in $[CuCl_4]^{2-}$. (a) Normalized K pre-edge peak heights from Ref. [14]. Reproduced with permission from Elsevier. (b) Oscillator strengths calculated using the exact semiclassical light-matter interaction with different symmetries.

symmetrically placed points is negligible and a numerical zero is observed at 180°, as it should be. Comparing the values for D_{2h}, D_{4h}, and $D_{2h\perp}$ directly, the difference is still below the accuracy of the calculation and discerning between D_{4h} and $D_{2h\perp}$ is not possible with the geometry differences here chosen.

C. Stability of K pre-edge XAS intensities of $[FeCl_4]^{1-}$

$[FeCl_4]^{1-}$ has a tetrahedral ligand environment. In T_d symmetry, the metal $3d$ orbitals belong to the e and t_2 irreducible representations, see Fig. 1. The iron $4p$ orbitals also have t_2, which means that they can mix through the interactions with the Cl ligands. The first two pre-edge transitions are to the $3d(e)$ orbitals and are electric dipole forbidden. The next three are to the t_2 orbitals, and they are more intense as they are electric-dipole allowed through the $4p$ mixing and get large contributions from several orders in the multipole expansion [8,15,21]. Not only will the electric quadrupole $f_{0n}^{(Q^2)}$ term be large, but the electric dipole $f_{0n}^{(\mu^2)}$ will be very large and the electric dipole electric octupole $f_{0n}^{(\mu O)}$ term will also be significant, even when the coordinate system is placed on the Fe atom.

TABLE I. The oscillator strength around 135° and 180° for $[CuCl_4]^{2-}$ in different symmetries. Numerals in square brackets represent the power of 10.

Angle	D_{2h}	D_{4h}	$D_{2h\perp}$
130	0.13423083[–04]	0.13417817[–04]	0.13415988[–04]
135	0.13832984[–04]	0.13834993[–04]	0.13833106[–04]
140	0.13408657[–04]	0.13417818[–04]	0.13415986[–04]
175	0.40993408[–06]	0.41717685[–06]	0.41711848[–06]
180	0.32151105[–10]	0.16725576[–17]	0.10545833[–16]
185	0.42435937[–06]	0.41717540[–06]	0.41711978[–06]

In previous applications that examined the origin independence of the multipole expansion in a mixed gauge, certain transitions in $[FeCl_4]^{1-}$ gave negative oscillator strengths at the second order, despite the fact that the zeroth order in the multipole expansion of the oscillator strengths should be the dominant term [8]. The strong negative oscillator strengths, however, only appeared in the cc-pVDZ and AUG-cc-pVDZ basis sets but not in the ANO-RCC basis sets. Since the oscillator strengths for the exact operator are inherently positive, it would therefore be interesting to see what values the multipole expansion should converge to, and second, to make a comparison of the numerical stability and performance of the exact operator and the multipole expansion.

In Table II the total dipole, quadrupole, and exact intensities for the transition from the ground to selected core-excited states in $[FeCl_4]^{1-}$ are shown in the ANO-RCC-VTZP and AUG-cc-pVDZ basis sets. The $G \rightarrow C1$ transition reaches the $3d(e)$ orbital, while both C3 and C5 are $3d(t_2)$ final states. C12 is a two-electron excitation, with both core and valence electrons excited simultaneously, and is typically weaker than the main transitions.

For the $G \rightarrow C1$ transition, the second-order contributions ($f_{0n}^{(2)}$) dominate the multipole expansion and the electric dipole $f_{0n}^{(\mu^2)}$ approach numerical noise, see Table II. The total oscillator strengths in the multipole expansion are then rather similar in the two basis sets. Instead, looking at the C3 and C5 transitions, they have large $f_{0n}^{(\mu^2)}$ contributions, which should lead to more intense transitions than for C1. However, the presence of large electric dipole contributions leads to large and unstable second-order contributions, even to the point where the total oscillator strength becomes negative for the AUG-cc-pVDZ basis set. Finally, the C12 transition illustrates that even if the total oscillator strength is positive, the multipole expansion leads to unphysical negative second-order contributions [8].

TABLE II. The total dipole- and quadrupole, second-order and exact oscillator strengths for the transition from the ground (G) to selected core-excited (CX) state in $[FeCl_4]^{1-}$ without spin-orbit coupling. The second order (Total) is the sum of the electric dipole $f_{0n}^{(\mu^2)}$ and the second-order contribution $f_{0n}^{(2)}$ of the multipole expansion. The dipole is given in both the length gauge $f_{0n}^{(\mu^2)}$ and velocity gauge $f_{0n}^{(\mu^2)^p}$. Numerals in square brackets represent the power of 10.

Basis	Transition	$f_{0n}^{(\mu^2)}$	$f_{0n}^{(\mu^2)^p}$	$f_{0n}^{(2)}$	Total	Exact
ANO-RCC-VTZP	$G \rightarrow C1$	0.157[–12]	0.151[–12]	0.407[–05]	0.407[–05]	0.371[–05]
AUG-cc-pVDZ	$G \rightarrow C1$	0.765[–06]	0.447[–06]	0.258[–05]	0.335[–05]	0.472[–05]
ANO-RCC-VTZP [8]	$G \rightarrow C3$	0.283[–04]	0.273[–04]	0.144[–05]	0.427[–04]	0.305[–04]
AUG-cc-pVDZ [8]	$G \rightarrow C3$	0.281[–04]	0.168[–04]	–0.585[–04]	–0.304[–04]	0.209[–04]
ANO-RCC-VTZP	$G \rightarrow C5$	0.283[–04]	0.273[–04]	0.144[–05]	0.427[–04]	0.305[–04]
AUG-cc-pVDZ	$G \rightarrow C5$	0.234[–04]	0.169[–04]	–0.539[–04]	–0.305[–04]	0.210[–04]
ANO-RCC-VTZP	$G \rightarrow C12$	0.555[–09]	0.419[–09]	–0.353[–09]	0.202[–09]	0.484[–09]
AUG-cc-pVDZ	$G \rightarrow C12$	0.730[–08]	0.627[–08]	0.752[–08]	0.148[–07]	0.624[–08]

Instead, looking at the results for the exact operator, the differences between the basis sets are significantly smaller, even for transitions where the second-order expansion gives total negative oscillator strengths. For transitions with strong dipole contributions, the exact operator is every time close to $f_{0n}^{(\mu^2)^p}$, which is not surprising since we use the exact operator in the velocity gauge and the integrand for the exact operator is closer to $f_{0n}^{(\mu^2)^p}$ than $f_{0n}^{(\mu^2)}$.

In the ANO-RCC-VTZP we see good agreement between the second-order and exact oscillator strengths. This is also reflected in the spectra, as seen in Fig. 3, where only minor differences in height of the peaks can be observed. Unlike for the multipole expansion, the peaks in the spectrum using the exact operator in the AUG-cc-pVDZ are now all positive. The better agreement between different basis sets could indicate that the exact operator is numerically more stable and reliable than the multipole expansion, though further numerical and theoretical investigation would be needed to conclude this. Studies along these lines are currently being undertaken.

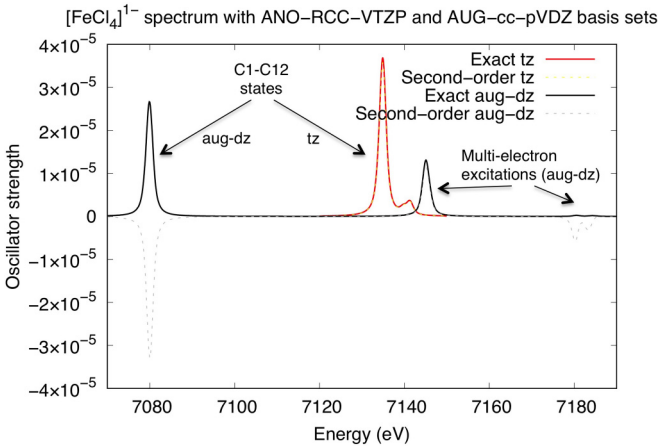

FIG. 3. A comparison of the spectra for $[FeCl_4]^{1-}$ using the exact operator and the second-order expansion in the AUG-cc-pVDZ and ANO-RCC-VTZP basis sets. Note that the spectra are energetically shifted due to different descriptions of the core orbitals. The spectra for the second order was previously published in Ref. [8].

D. Origin dependence of metal *K* pre-edge XAS of iron dimer

As shown by Bernadotte *et al.*, the full second-order expansion is origin independent in the velocity gauge [6,12]. We showed that this also holds in the true length gauge but not in the mixed gauge that is typically referred to as the length gauge [7,8]. This becomes an issue for an iron dimer that lacks a natural origin for the multipole expansion. As the individual iron sites in the dimer are asymmetric, metal $4p$ orbitals mix into the valence space, giving dipole-allowed transitions in the pre-edge, which leads to instability for the second-order expansion.

In [8] we showed that if the origin was placed close to the center of mass, the change in the spectrum for the so-called origin-independent quadrupole oscillator strengths in a mixed gauge was minor, while at slightly larger distances significant changes in the spectrum could be observed, see Fig. 4. The intensity of the second peak is most sensitive, which is consistent with larger electric-dipole contributions.

From Fig. 4 we see that the exact operator and the oscillator strengths in the mixed gauge agree rather well, both with respect to the shape and the total intensity of the spectrum. Previous *K* pre-edge calculations using the mixed gauge are therefore most likely of acceptable quality.

IV. PERSPECTIVE

While the results in Sec. III and implementation in Sec. II B does show that the exact semiclassical light-matter interaction is easier to implement and numerically better than the multipole expansion for the weak-field limit, we believe that the real strength of the approach lies in the strong-field regime.

A. Real-time-dependent light-matter interaction

For strong fields, where the perturbative treatment of the light-matter interaction breaks down, the multipole expansion is still used and the light-matter interaction is usually treated in the dipole approximation,

$$\hat{H} = \hat{H}_0 - \boldsymbol{E}(t)\boldsymbol{\mu}. \tag{33}$$

If the wave function is expanded in a Gaussian basis, then the exact same evaluation of the exact semiclassical light-matter interaction presented in Sec. II B could be used without any

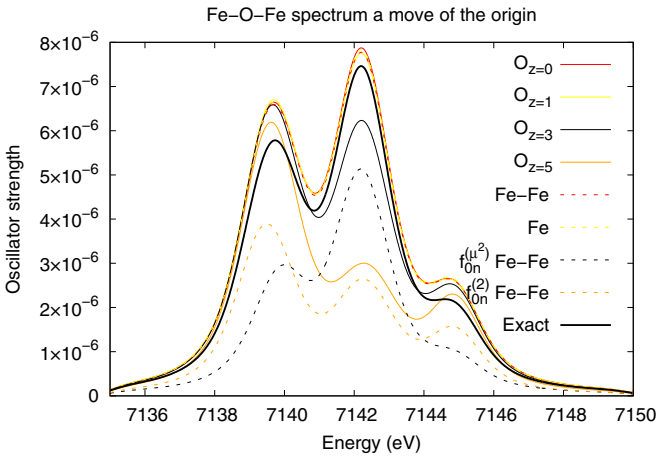

FIG. 4. A comparison of the spectra for Fe-O-Fe with the origin in the oxygen atom ($O_{x=0}$), origin moved along the x axis ($O_{x=d}$), where d is the distance, the origin in the middle between the two Fe atoms (Fe-Fe), and the origin placed on one of the Fe atoms (Fe) and the exact operator in the ANO-RCC-VTZP basis set. The $f_{0n}^{(\mu^2)}$ and $f_{0n}^{(2)}$ contributions are shown with the origin placed between the two Fe atoms. The data from the origin-independent quadrupole oscillator strengths in a mixed gauge is taken from Ref. [8].

significant added cost to a more general Hamiltonian,

$$\hat{H} = \hat{H}_0 + \hat{U}(t), \tag{34}$$

where $\hat{U}(t)$ is given by Eq. (2), to significantly improve the description of a laser pulse interacting with a target. Going beyond the dipole approximation is particularly interesting for x-ray spectroscopy, and in general, for very short wavelengths where the pulse varies over the size of the molecule, very strong time-dependent magnetic fields, and for multiphoton processes where the field becomes strong enough to see contributions from the $(\boldsymbol{A}^2)$ in Eq. (4). While the differences in oscillator strengths seem minor with well-behaving basis sets in the static case (see Fig. 4), these differences should quickly become apparent in the dynamic case, where it is the interaction with the laser field that drives the dynamics, since small initial differences in interaction can quickly grow large. In the real-time-dependent description the explicit strength and shape of the field would also have to be included, though these are merely the values of a time-dependent function describing the envelope and strength of the field.

V. CONCLUSION

We have presented a very easy way to implement the exact semiclassical light-matter interaction from Eq. (2), where the integrals either can be calculated analytically or extending the standard Gauss-Hermite integral evaluation to complex numbers. We show that the integral evaluation is akin to a Fourier transformation from real to k space of the overlap of the basis functions and that the electric, magnetic, and quadratic term $(\boldsymbol{A}^2)$ can be evaluated in the same way.

The main advantages of the exact operator is eightfold: (i) it is cheaper to calculate than higher-order terms in the multipole expansion for single directions, (ii) there are never negative oscillator strengths, (iii) it is always origin independent, (iv) it is easier to implement than higher orders in the multipole expansion, (v) it is easy to extend to time-dependent calculations, (vi) it appears to be more numerically stable, and (vii) it is less sensitive to the choice of basis set, since the basis set only has to work for a single type of integrand and not a multitude of different integrands as in the multipole expansion [9]. Additionally, (viii) using the exact operator also avoids the faulty interpretation of electric and magnetic terms in the multipole expansion, because this interpretation always will depend on the choice of coordinate system since none of these terms are observable. Finally, due to the ease with which the exact semiclassical light-matter interaction can be implemented, as well as the numerical, theoretical, and interpretation advantages, we do not see the need for using the multipole expansion anymore in the calculation of transition moments.

We show numerical examples of the exact operator on $[CuCl_4]^{2-}$ where the angle between beam and sample is known and on $[FeCl_4]^{1-}$ and Fe-O-Fe, where an isotropic averaging is performed. For the bis(creatinium)tetrachlorocuprate(II) crystal we have shown that with an angular-resolved spectrum we can discern the symmetry of the $[CuCl_4]^{2-}$ unit. The numerical stability of the exact operator, even in basis sets performing poorly for the multipole expansion, has been demonstrated for the $[FeCl_4]^{1-}$ molecule. In the AUG-cc-pVDZ basis set, even for transitions with negative second-order oscillator strengths the exact operator gave results close to those obtained for the exact operator in the better ANO-RCC-VTZP basis set, where the second-order oscillator strengths were positive. In fact, the difference between the oscillator strengths for the exact operator in the ANO-RCC-VTZP and AUG-cc-pVDZ basis sets is about the same as the difference between the exact operator and the second order in the ANO-RCC-VTZP basis set. The very good numerical performance of the exact operator, with respect to the basis size, seen in these preliminary calculations is currently being investigated. Finally for Fe-O-Fe we reproduce the spectrum previously published [8], which together with the results for $[FeCl_4]^{1-}$ in the ANO-RCC-VTZP basis shows that when good basis sets are used then the multipole expansion does produce results close to those of the exact operator.

While using the exact operator does give a significant improvement over the multipole expansion for weak fields, we do believe that the real strength of the approach will be in the dynamics of strong fields. We are therefore currently exploring the options of using the exact operator in time-dependent calculations, since this will give more accurate dynamics for molecules in strong laser fields, particularly for very short wavelengths, such as x rays, where the field varies over the range of the molecule or an atom, where terms above the dipole become important or where the $\boldsymbol{A}^2$ becomes important.

The implementation of the exact operator for electric and magnetic fields along with the integrals the for quadratic term $(\boldsymbol{A}^2)$ are freely available in OpenMolcas [30].

ACKNOWLEDGMENTS

Financial support was received from the Knut and Alice Wallenberg Foundation for the project Strong Field Physics and New States of Matter (Grant No. KAW-2013.0020)

and the Swedish Research Council (Grants No. 2012-3910, No. 2012-3924, and No. 2016-03398). Computer resources were provided by SNIC trough the National Supercomputer Centre at Linköping University (Triolith) under Projects No. snic2014-5-36, No. snic2015-4-71, No. snic2015-1-465, and No. snic2015-1-427.

[1] *Encyclopedia of Spectroscopy and Spectrometry*, edited by J. Lindon, G. E. Tranter, and D. Koppenaal, 3rd ed. (Academic Press, New York, 2016).

[2] B. P. Abbott, R. Abbott, T. D. Abbott *et al.* (LIGO Scientific Collaboration and Virgo Collaboration), Observation of Gravitational Waves from a Binary Black Hole Merger, Phys. Rev. Lett. **116**, 061102 (2016).

[3] *Springer Handbook of Atomic, Molecular, and Optical Physics*, Edited by G. W. F. Drake (Springer, Berlin, 2006).

[4] C. J. Joachain, M. Dörr, and N. Kylstra, High-intensity laser-atom physics, Adv. Mol. Opt. Phys. **42**, 225 (2000).

[5] J. H. Posthumus, The dynamics of small molecules in intense laser fields, Rep. Prog. Phys. **67**, 623 (2004).

[6] S. Bernadotte, A. J. Atkins, and C. R. Jacob, Origin-independent calculation of quadrupole intensities in X-ray spectroscopy, J. Chem. Phys. **137**, 204106 (2012).

[7] L. K. Sørensen, R. Lindh, and M. Lundberg, Gauge origin independence in finite basis sets and perturbation theory, Chem. Phys. Lett. **683**, 536 (2017).

[8] L. K. Sørensen, M. Guo, R. Lindh, and M. Lundberg, Applications to metal K pre-edges of transition metal dimers illustrate the approximate origin independence for the intensities in the length representation, Mol. Phys. **115**, 174 (2017).

[9] R. J. S. Crossley, The calculation of atomic transition probabilities, Adv. At. Mol. Phys. **5**, 237 (1969).

[10] N. H. List, J. Kauczor, T. Saue, H. J. Aa. Jensen, and P. Norman, Beyond the electric-dipole approximation: A formulation and implementation of molecular response theory for the description of absorption of electromagnetic field radiation, J. Chem. Phys. **142**, 244111 (2015).

[11] N. H. List, T. Saue, and P. Norman, Rotationally averaged linear absorption spectra beyond the electric-dipole approximation, Mol. Phys. **115**, 63 (2017).

[12] J. Lehtola, M. Hakala, A. Sakko, and K. Hämäläinen, ERKALE–A flexible program package for x-ray properties of atoms and molecules,J. Comp. Chem. **33**, 1572 (2012).

[13] G. Shulman, Y. Yafet, P. Eisenberger, and W. Blumberg, Observations and interpretation of x-ray absorption edges in iron compounds and proteins, Proc. Natl. Acad. Sci. USA **73**, 1384 (1976).

[14] J. E. Hahn, R. A. Scott, K. O. Hodgson, S. Doniach, S. R. Desjardins, and E. I. Solomon, Observation of an electric quadrupole transition in the x-ray absorption spectrum of a Cu(ll) complex, Chem. Phys. Lett. **88**, 595 (1982).

[15] T. E. Westre, P. Kennepohl, J. G. DeWitt, B. Hedman, K. O. Hodgson, and E. I. Solomon, A multiplet analysis of Fe K-Edge 1s $\rightarrow$ 3d Pre-Edge features of iron complexes, J. Am. Chem. Soc. **119**, 6297 (1997).

[16] J. Olsen, B. O. Roos, P. Jørgensen, and H. J. Aa. Jensen, Determinant based configuration interaction algorithms for complete and restricted configuration interaction spaces, J. Chem. Phys. **89**, 2185 (1988).

[17] P.-Å. Malmqvist, A. Rendell, and B. O. Roos, The restricted active space self-consistent-field method, implemented with a split graph unitary group approach, J. Phys. Chem. **94**, 5477 (1990).

[18] I. Josefsson, K. Kunnus, S. Schreck, A. Föhlisch, F. de Groot, P. Wernet, and M. Odelius, Ab initio calculations of x-ray spectra: Atomic multiplet and molecular orbital effects in a multiconfigurational SCF approach to the L-edge spectra of transition metal complexes, J. Phys. Chem. Lett. **3**, 3565 (2012).

[19] S. I. Bokarev, M. Dantz, E. Suljoti, O. Kühn, and E. F. Aziz, State-Dependent Electron Delocalization Dynamics at the Solute-Solvent Interface: Soft-X-ray Absorption Spectroscopy and Ab Initio Calculations, Phys. Rev. Lett. **111**, 083002 (2013).

[20] R. V. Pinjari, M. G. Delcey, M. Guo, M. Odelius, and M. Lundberg, Restricted active space calculations of L-edge x-ray absorption spectra: From molecular orbitals to multiplet states, J. Chem. Phys. **141**, 124116 (2014).

[21] M. Guo, L. K. Sørensen, M. G. Delcey, R. V. Pinjari, and M. Lundberg, Simulations of iron K pre-edge X-ray absorption spectra using the restricted active space method, Phys. Chem. Chem. Phys. **18**, 3250 (2016).

[22] M. Guo, E. Källman, L. K. Sørensen, M. G. Delcey, R. V. Pinjari, and M. Lundberg, Molecular orbital simulations of metal 1s2p resonant inelastic x-ray scattering, J. Phys. Chem. A **120**, 5848 (2016).

[23] F. V. Gubarev, L. Stodolsky, and V. I. Zakharov, On the significance of the vector potential squared, Chem. Phys. Lett. **86**, 2220 (2001).

[24] P. J. Lestrange, F. Egidi, and X. Li, The consequences of improperly describing oscillator strengths beyond the electric dipole approximation, J. Chem. Phys. **143**, 234103 (2015).

[25] M. Polášek and P. Čarsky, Efficient evaluation of the matrix elements of the coulomb potential between plane waves and gaussians, J. Comput. Phys. **181**, 1 (2002).

[26] P. Čarsky and M. Polášek, Evaluation of molecular integrals in a mixed gaussian and plane-wave basis by rys quadrature, J. Comput. Phys. **143**, 266 (1998).

[27] L. Füsti-Molnar and P. Pulay, Accurate molecular integrals and energies using combined plane wave and Gaussian basis sets in molecular electronic structure theory, J. Chem. Phys. **116**, 7795 (2002).

[28] A. J. Devaney and E. Wolf, Multipole expansions and plane wave representations of the electromagnetic field, J. Math. Phys. **15**, 234 (1974).

[29] P. Å. Malmqvist, Calculation of transition density matrices by nonunitary orbital transformations, Int. J. Quantum Chem. **30**, 479 (1986).

[30] https://gitlab.com/Molcas/OpenMolcas.

[31] P. Å. Malmqvist, B. O. Roos, and B. Schimmelpfennig, The restricted active space (RAS) state interaction approach with spin-orbit coupling, Chem. Phys. Lett. **357**, 230 (2002).

[32] R. Lindh, U. Ryu, and B. Liu, The reduced multiplication scheme of the Rys quadrature and new recurrence relations for auxiliary function based two-electron integral evaluation, J. Chem. Phys. **95**, 5889 (1991).

[33] L. D. Barron, *Molecular Light Scattering and Optical Activity*, 2nd ed. (Cambridge University Press, Cambridge, UK, 2004).

[34] V. I. Lebedev, Values of the nodes and weights of ninth to seventeenth order gauss-markov quadrature formulae invariant under the octahedron group with inversion, USSR Comput. Math. Math. Phys. **15**, 44 (1975).

[35] V. I. Lebedev, Quadratures on a sphere, USSR Comput. Math. Math. Phys. **16**, 10 (1976).

[36] V. I. Lebedev, Spherical quadrature formulas exact to orders 25–29, Sib. Math. J. **18**, 99 (1977).

[37] V. I. Lebedev and A. Skorokhodov, Quadrature formulas of orders 41, 47, and 53 for the sphere, Russ. Acad. Sci. Dokl. Math. **45**, 587 (1992).

[38] V. I. Lebedev, A quadrature formula for the sphere of 59th algebraic order of accuracy, Russ. Acad. Sci. Dokl. Math. **50**, 283 (1995).

[39] V. I. Lebedev and D. N. Laikov, A quadrature formula for the sphere of the 131st algebraic order of accuracy, Dokl. Math. **59**, 477 (1999).

[40] Z. Warnke, E. Styczeń, D. Wyrzykowski, A. Sikorski, J. Klak, and J. Mroziński, Structural and physico-chemical characteristics of tetraethylammonium tetrachloridoferrate (III), Struct. Chem. **21**, 285 (2010).

[41] M. Douglas and N. M. Kroll, Quantum electrodynamical corrections to the structure of helium, Ann. Phys. **82**, 89 (1974).

[42] B. A. Heß, Relativistic electronic-structure calculations employing a two-component no-pair formalism with external field projection operators, Phys. Rev. A **33**, 3742 (1986).

[43] B. O. Roos, R. Lindh, P.-Å. Malmqvist, V. Veryazov, and P.-O. Widmark, New relativistic ANO basis sets for transition metal atoms, J. Chem. Phys. **109**, 6575 (2005).

[44] B. O. Roos, R. Lindh, P.-Å. Malmqvist, V. Veryazov, and P.-O. Widmark, Main group atoms and dimers studied with a new relativistic ANO basis set, J. Phys. Chem. A **108**, 2851 (2004).

[45] P.-Å. Malmqvist and B. O. Roos, The CASSCF state interaction method, Chem. Phys. Lett. **155**, 189 (1989).